

1 **Genome scale mutational analysis of *Geobacter sulfurreducens* reveals distinct**  
2 **molecular mechanisms for respiration of poised electrodes vs. Fe(III) oxides**

3  
4  
5  
6  
7  
8  
9  
10  
11  
12  
13  
14  
15  
16  
17  
18  
19  
20  
21 Chi Ho Chan<sup>a</sup>, Caleb E. Levar<sup>a,b</sup>, Fernanda Jiménez-Otero<sup>a,c</sup>, Daniel R. Bond<sup>a,b,c</sup>

22  
23  
24 BioTechnology Institute<sup>a</sup>, Department of Microbiology<sup>b</sup>, and Department of Biochemistry,  
25 Molecular Biology, and Biophysics<sup>c</sup>, University of Minnesota-Twin Cities, Saint Paul MN 55108

26  
27  
28  
29 **Short title: Tn-Seq in *Geobacter***

30  
31  
32  
33  
34  
35  
36  
37  
38  
39  
40  
41 **Send all correspondence to:**

42  
43 Daniel R. Bond  
44 140 Gortner Laboratory  
45 1479 Gortner Ave  
46 St. Paul, MN 55108  
47 dbond@umn.edu

48  
49 **Keywords:** *Geobacter*, extracellular electron transfer, Tn-Seq, multiheme cytochrome

50

51 **Abstract**

52

53 *Geobacter sulfurreducens* generates electricity by coupling intracellular oxidation of organic  
54 acids with electron transfer to the cell exterior, while maintaining a conductive connection to  
55 electrode surfaces. This unique ability has been attributed to the bacterium's capacity to also  
56 respire extracellular terminal electron acceptors that require contact, such as insoluble metal  
57 oxides. To expand the molecular understanding of electricity generation mechanisms, we  
58 constructed *Geobacter sulfurreducens* transposon mutant (Tn-Seq) libraries for growth with  
59 soluble fumarate or an electrode surface as the electron acceptor. Mutant libraries with over  
60 33,000 unique transposon insertions and an average of 9 transposon insertions per kb allowed  
61 identification of 1,214 genomic features essential for growth with fumarate, including over 270  
62 genes with one or more functional homologs that could not be resolved by previous annotation  
63 or *in silico* modeling. Tn-Seq analysis of electrode-grown cells identified mutations in over 50  
64 genes encoding cytochromes, processing systems for proline-rich proteins, sensory systems,  
65 extracellular structures, polysaccharides, metabolic enzymes and hypothetical proteins that  
66 caused at least a 50% reduction in apparent growth rate. Scarless deletion mutants of genes  
67 identified via Tn-Seq revealed a new putative *c*-type cytochrome conduit complex (*extABCD*)  
68 essential for growth with electrodes, which was not required for Fe(III)-oxide reduction. In  
69 addition, mutants lacking components of a putative methyl-accepting chemotaxis/cyclic  
70 dinucleotide sensing network (*esnABCD*) were defective in electrode growth, but grew normally  
71 with Fe(III)-oxides. These results suggest that *G. sulfurreducens* possesses distinct  
72 mechanisms for recognition, colonization, and reduction of electrodes compared to other  
73 environmental electron acceptors.

74

75

76 **Importance**

77

78 Many metal-reducing organisms can also generate electricity at anodes. Because metal oxide  
79 electron acceptors are insoluble, one hypothesis is that cells sense and reduce metal particles  
80 using the same molecular mechanisms used to form biofilms on electrodes and produce  
81 electricity. However, by simultaneously comparing thousands of *Geobacter sulfurreducens*  
82 transposon mutants undergoing electrode-dependent respiration, we discovered new  
83 cytochromes and chemosensory proteins essential for growth with electrodes that are not  
84 required for metal respiration. This supports an emerging hypothesis where *G. sulfurreducens*  
85 recognizes surfaces and forms conductive biofilms using sensing and electron transfer  
86 pathways distinct from those used for growth with metal oxides. These findings provide a  
87 molecular explanation for studies that correlate electricity generation on electrode surfaces with  
88 direct interspecies electron transfer rather than metal reduction by *Geobacter* species, and  
89 reveal many previously unrecognized targets for improving and engineering this  
90 biotechnologically useful capability in other organisms.

91

## 92 Introduction

93

94 While most electron acceptors are soluble and easily reduced by inner membrane respiratory  
95 proteins, some electron acceptors are insoluble or lie beyond the cell surface. Bacteria able to  
96 catalyze 'extracellular electron transfer' or 'extracellular respiration' contain redox proteins and  
97 attachment mechanisms able to create electrical connections between membranes and these  
98 external substrates. Multiple modes of extracellular respiration are known, including reduction of  
99 Fe(III) and Mn(IV) oxides (1, 2), electricity production at electrode surfaces (3, 4), and formation  
100 of between-cell conductive networks enabling syntrophic growth with electron-consuming  
101 methanogens (5, 6).

102

103 The facultative anaerobe *Shewanella oneidensis* uses a single pathway comprised of the CymA  
104 inner membrane cytochrome and the MtrABC porin-multiheme *c*-type cytochrome complex to  
105 deliver electrons to all tested external metals and electrodes (7, 8). In contrast, there is evidence  
106 for multiple levels of complexity in the respiratory chain of the anaerobe *Geobacter*  
107 *sulfurreducens*. *G. sulfurreducens* requires two different inner membrane *c*-type cytochromes,  
108 ImcH and CbcL, depending on the reduction potential of the extracellular acceptor (9, 10). Up to  
109 five homologs of the PpcA periplasmic tri-heme *c*-type cytochrome could be involved in  
110 assisting electron transfer across the periplasm (11). To cross the outer membrane, one  
111 electron transfer 'conduit' complex consisting of the OmaB multiheme *c*-type cytochrome, OmbB  
112 porin-like protein, and OmcB multiheme lipoprotein *c*-type cytochrome is essential for growth  
113 with some metals (12, 13), but the genome encodes at least five other putative porin-  
114 cytochrome complexes with unknown functions. At the outer surface, *Geobacter* must build a  
115 conductive interface to reach metal particles, electrode surfaces, or partner bacteria. Simple  
116 extracellular polysaccharides influence biofilm interactions (14), while a combination of  
117 conductive Type IV pili and multiheme *c*-type cytochromes such as OmcS, OmcE, OmcZ and

118 PgcA are implicated in electron transfer beyond the cell membrane, depending on growth  
119 conditions (12, 14–16).  
120  
121 Due to the ease of screening mutants in liquid medium, compared to growth on electrodes in  
122 electrochemical reactors, most components of the *Geobacter* electron transfer pathway are  
123 identified using metals as proxies for other extracellular acceptors (14). Transposon-based  
124 mutagenesis using metals has revealed crucial cytochromes and attachment strategies, but  
125 high-throughput colorimetric screens are designed to identify mutants with growth rates near  
126 zero. Unfortunately, as multiple overlapping electron transfer pathways exist and many electron  
127 transfer proteins have functional homologs, single mutations typically decrease rather than  
128 eliminate growth of *G. sulfurreducens* (17, 18). This respiratory complexity, combined with the  
129 bottleneck of studying electron transfer in electrode biofilms, severely limits the pace of  
130 discovery when studying the molecular basis of complex phenotypes such as electricity  
131 production.  
132  
133 Transposon-insertion sequencing, also known as Tn-Seq, is able to quantify the abundance of  
134 every mutant containing a transposon insertion within a library, without individual mutant  
135 isolation (19). Using Tn-Seq, it is possible to measure the effect every mutation has on growth  
136 rate, by comparing an insertion's abundance before and after a known number of generations.  
137 This method rapidly assessed gene essentiality under aerobic versus anaerobic growth in  
138 *Shewanella oneidensis*, revealed genes essential to different respiration strategies in  
139 *Rhodospseudomonas palustris*, and uncovered the essential gene set in the archaeon  
140 *Methanococcus maripaludis* (20–22). For this report, we constructed the first *G. sulfurreducens*  
141 Tn-Seq library, and used it to define over 1,200 genes essential for growth in minimal medium  
142 using a soluble electron acceptor. By then cultivating this same mutant library on electrode  
143 surfaces, a subset of over 50 additional genes that caused at least a 50% decrease in growth

144 rate was revealed. Surprisingly, mutants lacking these new key cytochromes or chemosensory  
145 genes were severely impaired in growth with electrodes, but remained fully able to respire using  
146 other extracellular metal acceptors. These results suggest that separate biochemical  
147 mechanisms are used for electron transfer to electrodes and to environmental metals.

148

## 149 **Results and discussion**

150

151

152 **Tn-Seq in *G. sulfurreducens*.** *G. sulfurreducens* transposon libraries were generated using a  
153 *mariner*-based transposon with directional type IIS MmI recognition sites engineered on both  
154 ends of the transposon insertion sequence (22, 23). As MmI cleaves chromosomal DNA 20  
155 base pairs from its recognition site, adapter ligation and amplification allows sequencing to  
156 identify most insertions and quantify each mutant's abundance (24). After three separate  
157 transposon libraries were constructed using fumarate as the electron acceptor, approximately  
158 50,000 individual colonies were recovered per library, and sequencing revealed between 30,000  
159 and 33,000 independent insertions in each library with no obvious hotspots or biases in  
160 coverage. The library representing the deepest coverage was used as the source for all  
161 experiments reported in this work.

162

163 When DNA from two separate cultures within the same library was extracted, digested with  
164 MmI, ligated to Illumina adaptors, amplified, and sequenced, 33,257 and 33,343 unique  
165 insertions were identified in the two replicates. Over 97% of insertions occurred within annotated  
166 features at an average density of 9 unique insertions per kb (25). Despite opportunities for  
167 bottlenecking and bias during each growth, extraction, labeling and sequencing step, the  
168 number of reads mapped per annotated feature was reproducible with a Pearson's coefficient of  
169 0.98 between the two culture replicates (Fig. 1A). When two independent cultures were further  
170 grown with poised electrodes as the electron acceptor, then separately recovered, extracted,

171 and labeled, the number of reads mapped per gene in each independent growth experiment  
172 was similarly reproducible with a Pearson's coefficient of 0.98 (Fig. 1B).

173

174 **Essential genes for growth using fumarate in *G. sulfurreducens*.** To predict genes  
175 important for growth with electrodes, genes required for growth in standard minimal medium  
176 with the electron acceptor fumarate were first determined, so they could be excluded from  
177 further analyses. Tn-Seq libraries were grown in liquid culture for 6 generations and sequenced  
178 to a depth of >40 M reads per culture replicate. At this depth, an average of 1,200 reads are  
179 obtained per insertion, and based on an average feature size in *G. sulfurreducens* of 0.95  
180 kb/feature, 10,200 reads are expected to map to each feature in the annotated genome.

181

182 Previous constraint-based modeling predicted that a set of 140 central metabolic and  
183 biosynthetic genes should be essential for growth using fumarate as the sole electron acceptor  
184 (26). The majority (>90%) of these predicted essential genes had less than 300 mapped reads  
185 in our Tn-Seq analysis, compared to an expected 10,200 reads/gene, or they contained less  
186 than 4 insertions per kb (Fig. 2, Table S2). A small subset of genes previously predicted to be  
187 essential *in silico* averaged over 8,100 reads/feature and 10 insertions per kb, similar to other  
188 non-essential genome regions, and were considered to be non-essential under our growth  
189 conditions. Based on these results, annotated features with less than 300 reads mapped per  
190 feature or 4 insertion sites per kb were categorized as essential. Using both criteria allowed  
191 correction for small genes with few transposon insertion sites (TA dinucleotide) as well as larger  
192 genes which can support insertions between domains (27). According to this cutoff, over 170  
193 genes previously coded as non-essential in the *in silico* model were essential in our minimal  
194 medium. Most of these encoded biosynthetic pathways for biotin, riboflavin, and cobamide, as  
195 our medium lacked vitamins. In addition, biosynthesis pathways for heme, fatty acids, and  
196 lipopolysaccharides, along with putative transporters for sulfate, acetate, copper, cobalt, and

197 magnesium were essential. Complete tables comparing *in silico* predictions with Tn-Seq results  
198 are in Tables S3-S4.

199  
200 In total, almost 40% of annotated features, or 1,214 genome features out of 3,706, were  
201 identified as essential for growth with acetate as the electron donor and fumarate as the sole  
202 electron acceptor. A key difficulty in the original *G. sulfurreducens* annotation and *in silico*  
203 metabolic model was that genes encoding homologs or redundant pathways were not assigned  
204 function, as they could possibly complement each other (18, 19). Tn-Seq analysis clarified  
205 hundreds of such issues. For example, despite the presence of five annotated ferredoxins, only  
206 one was essential (GSU2708), one of three 2-oxoglutarate dehydrogenase complexes was  
207 essential (GSU1467 – GSU1470), one of three aconitase enzymes was essential (GSU1660),  
208 one of two fructose biphosphate aldolases was essential (GSU1193), and two of three  
209 phosphoglycerate mutase enzymes were essential (GSU1818 and GSU3207). In total, Tn-seq  
210 resolved the essentiality of over 270 such examples where homologs were present but only  
211 specific genes were required under laboratory conditions (Table S5-S6).

212  
213 Of special interest in *Geobacter* electron transfer is the mechanism of NADH oxidation and  
214 electron delivery to the quinone pool. This remains poorly understood, partially due to the fact  
215 that most *Geobacteraceae* encode two distinct complex I-NADH dehydrogenases (28). The  
216 complex I similar to that found in other Proteobacteria, recently classified as type “E” (GSU3429  
217 – GSU3445) was not essential in *G. sulfurreducens*. However, a second, less well characterized  
218 complex I was essential. This NADH dehydrogenase does not fall into a major defined clade,  
219 and is most closely related to complex I sequences in *Chloroflexi* (GSU0338 – GSU0351) (28).  
220 A second essential gene cluster with bioenergetic implications was an integral membrane *b*-type  
221 cytochrome/FeS cluster/electron transfer flavoprotein. These genes (GSU2795 – GSU2797)  
222 encode all signature residues of confurcation/bifurcation complexes, suggesting high and low



223 potential electrons (such as NADH + reduced Fd) may be combined for quinone pool reduction  
224 or proton translocation events during oxidation of acetate (29).

225

226 **Genes affecting electrode growth of *G. sulfurreducens*.** Growth on an electrode surface in  
227 microbial fuel cells and electrochemical devices is hypothesized to be a complex phenotype that  
228 requires attachment, movement of electrons across membranes, and formation of between-cell  
229 conductivity to sustain respiration by cells not in contact with the surface (9, 10, 14, 30, 31). To  
230 test the entire process from attachment to biofilm growth, two parallel Tn-Seq libraries were  
231 grown for 6 generations on an electrode poised at -0.1 V vs. Standard Hydrogen Electrode  
232 (SHE), and the density of reads mapped per feature compared to parallel fumarate-grown cells.  
233 The electrode potential (-0.1 V vs. SHE) was chosen to mimic the redox potential of  
234 environmental Fe(III) oxides (32).

235

236 Expressing Tn-Seq read density data as  $\text{Log}_2$  ratios allows quick assessment of a phenotype.  
237 For example, a mutation preventing growth in a mutant results in twice as many wild type reads  
238 after one generation, or a  $\text{Log}_2$  ratio of -1. Using the exponential growth equation, genes with a  
239  $\text{Log}_2$  score of -2 after 6 generations are equivalent to at least a 50% reduction in apparent  
240 doubling time. Using this criteria, nearly 50 genes encoding cytochromes, protein processing  
241 systems, sensing proteins, extracellular structures, polysaccharides, metabolic enzymes and  
242 hypothetical proteins were involved in electrode growth. Full data showing all read mapping  
243 densities and  $\text{Log}_2$  ratios for all features is in Table S2, and all raw read data needed to re-  
244 create this analysis is available in NCBI BioProject PRJNA290373. Direct links for downloading  
245 read mapping files and the annotated genome for viewing in IGV is in file S7.

246

247 Tn-Seq analysis confirmed a previous finding that CbcL, an inner membrane putative quinone  
248 oxoreductase containing both *b*- and *c*-type cytochromes (GSU0274) is crucial for electrode

249 growth when electrodes are poised at -0.1 V vs. SHE (9, 10). Insertions in *cbcL* resulted in Log<sub>2</sub>  
250 ratios corresponding to doubling times of 17.4 h, while a ~20 h doubling time was previously  
251 estimated for a pure culture  $\Delta cbcL$  mutant (9). Also in agreement with previous work was the  
252 severe negative impact of insertions in genes involved in assembly and expression of the  
253 conductive Type VI pili. Insertions in the *pilQPOM* operon (GSU2028 – GSU2032), *pilC* gene  
254 (GSU1493) and *pilS* sensor kinase (GSU1494) produced similar defects, while insertions in  
255 other Type VI pili genes predicted weaker phenotypes (below the threshold in Table 2), but still  
256 causing at least a 25% decrease in apparent growth rate. Insertions in some pili genes, such as  
257 the *pilT4* gene (GSU1492), led to increased apparent abundance, consistent with recent reports  
258 that pilT mutants more rapidly colonize electrodes (33).

259  
260 Surprisingly, with the exception of CbcL, no other cytochromes reported to play a role in  
261 electron transfer to metals appeared to be required for growth with an electrode in the Tn-Seq  
262 analysis. Instead, insertions in two uncharacterized multiheme c-type cytochromes did  
263 significantly affect electrode growth (GSU2643 and GSU2645). These cytochromes are part of a  
264 cluster containing two multiheme c-type cytochromes, a multiheme lipoprotein cytochrome, and  
265 a predicted outer membrane porin-like protein. As a similar arrangement of multiheme  
266 cytochromes, lipoprotein cytochromes, and putative  $\beta$ -barrel proteins encodes a “conduit” for  
267 electron transfer across the outer membrane in both *Geobacter* (the OmcB-based conduit) and  
268 *Shewanella* (the MtrCAB conduit), this region was targeted for further study.

269  
270 The *G. sulfurreducens* genome encodes over 100 histidine kinases, response regulators and  
271 chemotaxis-like proteins, yet little is known about their role controlling phenotypes such as  
272 extracellular respiration (34). Tn-Seq identified one DNA-binding protein (GSU0013), and four  
273 chemotaxis proteins (GSU1704 and GSU2220 – GSU2222) as significant at the level of a 50%  
274 growth reduction. Only one diguanylate cyclase-response regulator protein was suggested to

275 participate in electrode-dependent growth (GSU3376) above the level of a 25% reduction in  
276 growth. In model systems, methyl-accepting chemotaxis proteins such as GSU1704 undergo a  
277 conformational change to interact with CheW (GSU2220) and CheA (GSU2222) family proteins,  
278 triggering phosphorylation of GSU3376-like response regulators (35). Based on the hypothesis  
279 that GSU1704, GSU2220, GSU2222 and GSU3376 represented portions of MCP-CheA-CheW-  
280 response regulator systems involving the biofilm regulator c-di-GMP, these were also targeted  
281 for further study.

282  
283 Some of the strongest phenotypes in apparent electrode growth were due to insertions in genes  
284 encoding sugar and polysaccharide synthesis. Five different sugar dehydrogenases, sugar  
285 transferases, and isomerases were identified as being required for electrode growth via Tn-Seq,  
286 and insertions within at least three different gene clusters involved in capsule,  
287 lipopolysaccharide and extracellular sugar synthesis produced significant defects. Also crucial  
288 were genes putatively involved in translocating sugars to the outer surface, such as a sugar  
289 ABC transporter previously shown to be essential for electrode growth (*xapD*, GSU1501), and  
290 an LPS ABC transporter protein (*lptA*, GSU1889). The defects created by these insertions  
291 further support a role for sugars in creating a properly charged or modified outer surface during  
292 *Geobacter* biofilm formation on electrodes (14, 16).

293  
294 Finally, proteins involved in translation and processing of proline-rich proteins became important  
295 during electrode growth. For example, elongation factor P is essential for overcoming ribosome  
296 stalling during translation of proline-repeat sequences, and contributes to outer membrane  
297 integrity in *E. coli* (36, 37). Tn-Seq analysis predicted that one of two Ef-P homologs in *G.*  
298 *sulfurreducens*, (Efp-2, GSU1752), along with the Ef-P modifying Ef-P lysine-lysyltransferase  
299 (GSU1753) and Ef-P lysyl-lysine 2,3-aminomutase (GSU1754) became important during growth  
300 with electrodes. Insertions in a prolidase involved in cleaving peptides at proline residues (GSU

301 1105) and peptidylprolyl cis-trans isomerase (GSU2074) showed strong growth defects, further  
302 suggesting an unrecognized importance in the folding and processing of proline-rich proteins  
303 under electrode respiring conditions.

304

305 **Possible genes missed by the community aspect of Tn-Seq analysis.** Deletion of the outer  
306 surface cytochrome gene *omcZ* (GSU2076) can significantly decrease electrode growth (38).  
307 While Tn-Seq insertions in genes within the *omcZ* operon had a negative impact (such as the  
308 peptidylprolyl cis-trans isomerase, GSU2074), insertions in *omcZ per se* were not identified as  
309 causing a defect in our library experiments (38, 39). Similarly, the pili-associated cytochrome  
310 OmcS is reported to be involved in electron transfer to electrodes, yet it was not identified in our  
311 analysis. Both of these cytochromes are verified to exist beyond the cell membrane, in the  
312 conductive matrix between cells (39, 40).

313

314 Under Tn-Seq conditions, enzymatic activities and proteins can be shared. A clear example of  
315 population-based complementation was evident in Tn-Seq data for fumarate hydratase, a TCA  
316 cycle gene predicted *in silico* to be absolutely essential (GSU0944, Table S3). Due to the fact  
317 that wild type *G. sulfurreducens* secretes malate when grown with fumarate as the electron  
318 acceptor (41), we hypothesized that fumarate hydratase was not required by the small  
319 subpopulation of fumarate hydratase mutants, as extracellular malate can rescue the gap in the  
320 TCA cycle. Consistent with this hypothesis, during growth with an electrode in the absence of  
321 fumarate, fumarate hydratase became one of the most essential genes in Tn-Seq analysis.

322

323 Our data suggest that extracellular cytochromes such as OmcZ secreted by wild type cells may  
324 similarly aid the occasional  $\Delta omcZ$  mutant in the biofilm population during Tn-Seq experiments.  
325 This phenomenon would be similar to how outer membrane proteins shared between  
326 *Myxococcus* strains rescue motility mutants (42), and siderophores act as “public goods” for

327 rare non-producing strains (43). In contrast to evidence that OmcS and OmcZ might be shared  
328 between cells, cellular machinery such as the Type IV pili, inner membrane cytochromes and  
329 outer membrane cytochromes remained essential even in biofilm conditions. Further Tn-Seq  
330 experiments may provide a mechanism to discover which *Geobacter* extracellular proteins can  
331 be shared for communal conductivity and exploited by 'cheaters' embedded in a conductive  
332 matrix, vs. which proteins catalyze key attachment or electron escape reactions so essential to  
333 each cell that they cannot be borrowed from neighbors.

334  
335 **Cytochrome conduit deletion mutants affect electrode- but not Fe(III)-reduction.** While Tn-  
336 Seq agreed with the importance of previously reported mechanisms such as pili, inner  
337 membrane cytochromes, and extracellular sugars, it identified many processes never  
338 highlighted in any mutant, proteomic, or transcriptional study. Based on their strong phenotypes  
339 under Tn-Seq conditions, we investigated the roles of two surprising classes of mutants,  
340 involving new outer membrane cytochromes and signaling proteins, after constructing scarless  
341 deletions of these key genes and gene clusters.

342  
343 In Tn-Seq data, no effect was observed for mutations in one of the most studied outer  
344 membrane c-type cytochromes in *G. sulfurreducens*, OmcB. Part of a trans-outer membrane  
345 porin-cytochrome conduit capable of transferring electrons across the outer membrane, OmcB  
346 is encoded in a three-gene cytochrome/porin-like protein/lipoprotein cytochrome cluster (*ombB*-  
347 *omaB-omcB*, GSU2737–GSU2739) located next to a nearly identical tandem duplication  
348 containing another conduit (*ombC-omaC-omcC*, GSU2731–GSU2733). This duplication limits  
349 the impact of single mutations in any one gene. Thus, a scarless deletion of this entire genomic  
350 region, lacking all genes in the *omcB* and *omcC*-encoded conduits was constructed, and is  
351 referred to here as  $\Delta omcBC$  ( $\Delta$ GSU2739 – GSU2731). Genes for a new putative porin-  
352 cytochrome conduit, that shares no homology with the OmcB or OmcC conduits, showed a

353 strong phenotype in Tn-Seq data. This conduit was termed *extABCD* (extracellular electron  
354 transfer) and genes were removed to generate the  $\Delta extABCD$  ( $\Delta$ GSU2645-GSU2642) strain. In  
355 addition, deletion mutants of two other putative outer membrane conduit clusters,  $\Delta extEFG$   
356 (GSU2726 – GSU2724) and  $\Delta extHIJKL$  (GSU2940 – GSU2936) were constructed as controls to  
357 compare with Tn-Seq results.

358

359 The  $\Delta extABCD$  strain grew poorly when the electrode was the electron acceptor, never  
360 producing more than 50  $\mu\text{A}/\text{cm}^2$  when grown under the same conditions used for Tn-Seq. In  
361 contrast, the  $\Delta omcBC$  deletion strain showed no defect, and grew on the electrode similar to  
362 wild type (Fig. 3A). The other mutants lacking outer membrane conduits,  $\Delta extEFG$  and  
363  $\Delta extHIJKL$ , also showed no defects on the electrode, demonstrating similar growth rates and  
364 final current densities as wild type. All mutants grew with wild type growth rates using fumarate  
365 as the electron acceptor, as predicted by Tn-Seq essentiality data (data not shown). While  
366 single-gene replacement mutants lacking the *omcB* gene will grow in microbial fuel cells (44),  
367 these results demonstrated that no part of the *ombB-omaB-omcB* and/or *ombC-omaC-omcC*  
368 conduit genes were required for wild type colonization and reduction of electrodes. Two other  
369 putative trans-outer membrane conduit gene clusters are also not essential for electron transfer  
370 to electrodes. In both Tn-Seq and in pure culture studies with reconstructed mutants, only the  
371 deletion of *extABCD* had any effect when electrodes were the electron acceptor.

372

373 In contrast to the strong electrode phenotype observed for the mutant lacking *extABCD*,  
374 reduction of insoluble Fe(III)-oxide by  $\Delta extABCD$  was unaffected. Even though metal oxide  
375 particles are surfaces with similar redox potentials as the electrodes used in the Tn-Seq  
376 analysis, the *extABCD* gene cluster was not essential for reduction of metals (Fig. 3B). The  
377 phenotype of the  $\Delta extABCD$  mutant suggests that the dominant pathway of electron transfer

378 across the outer membrane will vary, based on what is being used as the extracellular electron  
379 acceptor.

380

381 **Chemosensory system deletion mutants also affect electrode- but not Fe(III)-reduction.** A

382 second class of genes revealed by Tn-Seq analysis were related to intracellular sensing and  
383 signaling systems. Based on their Tn-Seq phenotypes, these proteins were termed part of an  
384 electrode sensing network, and included; EsnA, a methyl-accepting chemotaxis protein  
385 (GSU1704), EnsB, a CheW-like chemotaxis scaffolding protein (GSU2220), EsnC, a CheA-like  
386 chemotaxis histidine kinase (GSU2222), and EsnD, a diguanylate cyclase (GSU3376). Scarless  
387 deletion mutants of each *esn* gene were constructed and tested for growth using an electrode  
388 as the electron acceptor.

389

390 All four *esn* deletion mutants displayed defects in growth with an electrode even more severe  
391 than the Log<sub>2</sub> ratios observed in Tn-Seq data (Fig. 3A and Table 2). However, when these same  
392 four *esn* mutants were grown with Fe(III)-oxide as the electron acceptor, Fe(III) reduction was  
393 similar to wild type (Fig. 3B). All mutants also grew at wild type growth rates with fumarate as  
394 the electron acceptor. This phenotype, where a mutant performed poorly with an electrode  
395 surface but still reduced metal oxide particles, agreed with the hypothesis that cells interact with  
396 these two solid-phase electron acceptors via different molecular mechanisms.

397

398 Further work will be required to determine if the similar phenotypes displayed by *esn*-encoded  
399 proteins is due to direct physical interactions or common signaling molecules. No annotated  
400 MCP genes in the *G. sulfurreducens* genome are co-localized in operons with a complete set of  
401 CheA-CheW genes, and no protein-protein interaction data is available to predict the  
402 downstream target of the EsnC CheA-like kinase. The EsnA methyl-accepting chemotaxis  
403 protein has no periplasmic sensing domain to suggest an external input for this system, but

404 EsnA does contain a cytoplasmic GAF domain typically involved in binding small molecules  
405 such as cyclic nucleotides, and EsnD is a demonstrated cyclic-di-GMP producing response  
406 regulator (45). One hypothesis is that EsnABC together regulates and/or responds to levels of  
407 EsnD-produced cyclic-di-GMP, driving and reinforcing a switch to the conductive biofilm mode  
408 of growth (46). Whatever the ultimate signal is for electrode colonization, it does not appear to  
409 be involved in growth with metals such as Fe(III).

410

411 **Conclusions and outlook.** The ability of Tn-Seq to survey mutants across the entire genome in  
412 a single growth experiment is especially useful when no high-throughput assay is available for  
413 the phenotype under study. In the case of growth on electrodes, testing 33,000 individual  
414 mutants in replicate electrode reactors would require our laboratory to dedicate its bank of 45  
415 electrochemical cells to testing mutants nonstop for over 28 years. In a fraction of that time,  
416 saturation mutagenesis described over 1,200 genes essential for growth under laboratory  
417 conditions, resolved hundreds of annotation issues, and brought into focus over 50 genes vital  
418 during electrode growth conditions.

419

420 By asking what genes are required for growth, Tn-Seq generates data different from expression-  
421 based approaches which operate under the hypothesis that important genes will be strongly  
422 regulated in response to an electrode. Transcriptional data did lead to discovery of the key  
423 multiheme cytochrome OmcZ in *Geobacter*, and supported early hypotheses suggesting a role  
424 for pili. However, microarrays also found strong up-regulation of many genes which failed to  
425 show importance in follow-up mutant studies, and failed to show phenotypes in these Tn-Seq  
426 results (38). Examples include; the OmcB and OmcC cytochromes and multiple hypothetical  
427 cytochromes, amino acid transporters and hydrogenases, terminal oxidases involved in oxygen  
428 reduction, and heavy metal exporters. In general, we found little overlap between genes  
429 predicted as important to growth on electrodes via Tn-Seq and those up- or down-regulated in



430 expression or proteomic studies on electrodes (31, 38, 47). One possibility is crucial regulatory  
431 or biosynthetic elements have low basal expression levels. Expression or abundance-based  
432 studies could have reduced sensitivity if biofilms are heterogeneous, or if expression varies with  
433 distance from the electrode (48). In the case of cytochromes, the *imcH* and *cbcL*-encoded  
434 cytochromes involved in electron transport are now known to be expressed even when cells are  
435 grown with fumarate, preventing their earlier discovery via differential expression (9, 10). It also  
436 remains possible that electrodes, being relatively unnatural substrates, trigger additional  
437 transcriptional changes or de-repress genes that have little to do with electrode respiration.

438  
439 Tn-Seq data provided genome-scale information that agreed with prior *in silico* predictions and  
440 knockouts during fumarate reduction (26, 49). However, much less data are available for  
441 electrodes in terms of what genes are essential, and as with any large-scale survey,  
442 reconstruction of mutants is needed to corroborate findings. Using scarless mutants lacking  
443 genes and whole gene clusters, we were able to confirm that individual chemosensory  
444 components of *esnABCD* and the entire cytochrome conduit *extABCD* were essential for growth  
445 when the electrode acted as the electron acceptor. As two other outer membrane conduits,  
446 based on OmcB and OmcC, are well-studied and known to be involved in electron transfer to  
447 metals, we also constructed new mutants lacking these non-homologous cytochrome clusters,  
448 along with two other unstudied putative outer membrane conduits. Surprisingly, only removal of  
449 the *extABCD* conduit gene cluster affected electrode growth, as predicted by Tn-Seq.

450  
451 When Fe(III) was the electron acceptor, none of the cytochrome conduit mutants with electrode  
452 phenotypes, and none of the mutants lacking methyl-accepting chemotaxis proteins or GGDEF-  
453 domain response regulators, had significant defects (Fig. 3B). These data support a model that  
454 *G. sulfurreducens* possesses separate mechanisms for reduction of electrodes compared to the  
455 reduction of metals that involves a distinct set of cytochromes for crossing the outer membrane.

456 In addition, separate cyclic dinucleotide-dependent regulatory systems may be used for  
457 recognition and respiration of electrodes compared to metals.

458  
459 A recent comparison of seven *Geobacter* species noted a poor correlation between electricity  
460 production and Fe(III) reduction rates (50). In contrast, strains capable of high rates of electricity  
461 production were also capable of interspecies electron transfer to methanogens. This correlation  
462 led to the hypothesis that the conductive network accessible to electrodes evolved to support  
463 direct electron transfer between *Geobacter* and electron-accepting organisms such as  
464 methanogens. Evidence for this hypothesis lies also in the use of anaerobic digesters as the  
465 most common source of high current-producing *Geobacter* enrichments (51), compared to  
466 Fe(III)-rich environments (50, 52). A syntrophic partner may be much like an electrode; it can  
467 accept electrons indefinitely, but requires commitment to an attached biofilm lifestyle and the  
468 expense of building a conductive extracellular space (6, 53). In contrast, small metal oxide  
469 particles represent a temporary and more variable electron acceptor, where cells cannot attach  
470 permanently or grow into thick biofilms that entrap and re-use extracellular proteins (54).

471  
472 While naturally-occurring *Geobacter* strains produce  $>1$  mA/cm<sup>2</sup> of electrical current, and this  
473 rate already rivals the best artificial enzyme-functionalized electrodes (55), use of microbial  
474 electrochemistry as an energy source or biocatalyst is estimated to require at least a 10-fold  
475 increase in current density in order to be profitable (56–58). Achieving these gains, and  
476 engineering these abilities into industrial bacteria, requires identification and enhancement of  
477 core components specific to electricity production. While the molecular basis for this  
478 extracellular respiration is becoming more clear, how organisms biochemically distinguish  
479 between insoluble metals vs. microbial or electrode-based acceptors remains a key challenge.

480 **Materials and Methods**

481

482 **Growth and medium conditions.** All strains and plasmids used in this study are listed in Table

483 1. *G. sulfurreducens* strains and mutants were grown from single colony picks streaked from lab

484 DMSO stocks in anoxic basal medium as described (59). For routine growth, basal medium with

485 acetate (20 mM) as the electron donor and fumarate (40 mM) as the electron acceptor was

486 used. Agar (1.5%) was added to the acetate-fumarate medium when culturing for clonal isolates

487 on semisolid surface in an H<sub>2</sub>:CO<sub>2</sub>:N<sub>2</sub> (5:20:75) atmosphere in a vinyl anaerobic chamber (Coy)

488 or an anaerobic workstation 500 (Don Whitley). When electrodes were used as the electron

489 acceptor, fumarate was replaced with 50 mM NaCl to maintain a similar ionic strength. When

490 Fe(III)-oxide was used as the electron acceptor, fumarate was omitted and a non-chelated

491 mineral mix was used (in which all components of the chelated mix were dissolved in a small

492 volume of 1N HCl without NTA). In all cases, the pH of the medium was adjusted to 6.8,

493 buffered with 2 g/L NaHCO<sub>3</sub> and purged with N<sub>2</sub>:CO<sub>2</sub> gas (80:20) passed over a heated copper

494 column to remove trace oxygen.

495

496 Three-electrode bioreactors were assembled as previously described (60). Briefly, graphite

497 electrodes were polished using 1,500 grit wet/dry sandpaper and attached to platinum wire to

498 serve as the working electrode. A bare platinum wire was the counter electrode. The potential

499 of the working electrode was maintained at -0.10 V vs. standard hydrogen electrode (SHE)

500 using a saturated calomel reference electrode and a VMP3 multichannel potentiostat (Biologic).

501 Reactor headspace was degassed using 80:20 N<sub>2</sub>:CO<sub>2</sub> prior to inoculation. Current was

502 measured as an average over two minutes. For all pure culture mutant experiments, a 25%

503 inoculum with cultures reaching acceptor limitation (OD<sub>600</sub>=0.50-0.55) was used. The total

504 volume of each reactor was 15 ml, and the working electrode surface area was 3 cm<sup>2</sup>.

505

506 To assay Fe(III) oxide reduction in *G. sulfurreducens*, late exponential growth phase cultures  
507 ( $OD_{600} = 0.5-0.55$ ) grown using acetate-fumarate were used to inoculate 1:100 in minimal  
508 medium containing 20 mM acetate as the electron donor and 55 mM freshly precipitated  $\beta$ -  
509 FeO(OH) as the sole electron acceptor. A small sample of the medium was removed at regular  
510 intervals and dissolved in 0.5 N HCl for at least 24 hours in the dark. The acid extractable Fe(II)  
511 was measured using a modified FerroZine assay (59).

512 *Escherichia coli* was cultivated in lysogeny broth supplemented with 0.3 M 2,3-diaminopimelic  
513 acid and 50  $\mu$ g/ml kanamycin when needed.

514  
515 **Tn-Seq library construction.** Five ml of mid-log ( $OD_{600} \sim 0.35$ ) *G. sulfurreducens* culture grown  
516 on acetate-fumarate was combined with 5 ml of an overnight culture of *E. coli* conjugative donor  
517 strain BW29427 (WM3064) carrying the transposon plasmid pEB001 was applied to a  
518 nitrocellulose filter (0.4  $\mu$ m pore size) using a vacuum. Plasmid pEB001 contains the *mariner*  
519 derivative *Himar1* transposon with Mmel recognition sites on both sides of the inverted repeats  
520 that flank a kanamycin resistance cassette. *G. sulfurreducens* recipient and *E. coli* donor  
521 mixture was washed on the filter with 3 volumes of basal medium before transferring the filter  
522 with the cell mixture to an agar plate containing acetate-fumarate and incubated in a Coy  
523 chamber at 30°C for 4 hours. The cell mixture was washed off the filter disc with 1 ml of basal  
524 medium supplemented with 200  $\mu$ g/ml kanamycin. To select for *G. sulfurreducens* transposon  
525 mutants, dilutions were plated on large 22 x 22 cm square agar plates with acetate-fumarate  
526 medium supplemented with kanamycin and incubated at 30°C in the anoxic chamber until  
527 visible colonies formed (in six days). Approximately 50,000 colonies were pooled in 10 ml of  
528 acetate-fumarate medium and grown for 4 hours before freezing 1 ml aliquots in 10% DMSO.

529  
530 **Tn-Seq experiment.** For each experiment, a frozen library aliquot was used to inoculate 100 ml  
531 of acetate-fumarate medium. When cultures reached exponential growth phase ( $OD_{600} \sim 0.35$ ), 5

532 ml of this culture was inoculated into fresh 100 ml acetate-fumarate medium. This parent culture  
533 was grown to early stationary phase ( $OD_{600} \sim 0.5$ ) and used to initiate both electrode and  
534 fumarate control experiments. Five ml of the parent culture was inoculated into 100 ml of  
535 acetate-fumarate medium and allowed to grow for 6 generations before harvesting. At the same  
536 time, a 7.5 ml of the parent culture was inoculated into the 3-electrode bioreactor containing 7.5  
537 ml of medium, where two 3 cm<sup>2</sup> working electrodes were present to support biofilm growth. *G.*  
538 *sulfurreducens* electrode biofilms were harvested by moving reactors to an anaerobic chamber  
539 after 6 generations of growth using electrodes poised at -0.1 V SHE, with the number of  
540 generations estimated based on the doubling time (10 h) at this redox potential. The entire  
541 electrode plus attached biofilm was placed in 100 ml of acetate-fumarate minimal medium,  
542 vortexed to liberate cells, and incubated at 30°C for 6 generations before harvesting. This  
543 outgrowth was necessary to produce adequate free biomass for DNA extraction and  
544 sequencing, and is why cells grown with fumarate for an additional 6 generations were used as  
545 a parallel control. Despite this additional outgrowth step, read densities and phenotypes  
546 between replicate experiments were highly repeatable (see Fig 1B).

547  
548 Genomic DNA from 40 ml of cells was isolated using the Wizard genomic DNA purification kit  
549 (Promega). The protocol for preparing the DNA library for Illumina sequencing is outlined with  
550 modifications (61). Six µg of gDNA was digested with MmeI (New England Biolabs) for 2 hours  
551 at 37°C. To this reaction, Antarctic phosphatase (New England Biolabs) was added and  
552 incubated at 37°C for an additional hour. Enzymes were inactivated at 65°C for 15 minutes,  
553 followed by phenol/chloroform/isoamyl acetate (25:24:1) extraction and ethanol precipitation at -  
554 20°C overnight. MmeI digested gDNA and Illumina barcoded adaptor with two random base pair  
555 overhangs were ligated using T4 DNA ligase (Epicentre) for 1 hour at 25°C. The transposon  
556 with 20 bp of genomic DNA sequence junction and ligated adaptor was amplified using Phusion  
557 High GC master mix (New England Biolabs) using primers (P1 M6 MmeI and Gex PCR Primer

558 2) that anneal to the inverted repeat of the transposon and the ligated Illumina adaptor. The  
559 PCR reaction was terminated during linear amplification (24). The 120 bp product was gel  
560 purified and saved at -20°C. After Sanger sequencing verification using primer Gex PCR Primer  
561 2 for the presence of the unique barcode, the PCR product was sequenced using Illumina  
562 (HiSeq 2500 Rapid chemistry single read 50 bp). Three samples with unique barcodes were  
563 mixed in a single Illumina lane generating ~30 M quality-passing reads per sample. All  
564 sequencing was performed by the University of Minnesota Genomics Center. Primers and  
565 barcoded adaptors used in the construction of the Tn-Seq library are referenced here (61).

566  
567 **Mapping of transposon insertions:** For each Tn-Seq library, raw sequences were de-  
568 multiplexed and extracted according to the unique barcode. The barcode and transposon  
569 sequences were trimmed, keeping only genome sequences that were at least 16 bp in length.  
570 Reads were then aligned to our *G. sulfurreducens* reference genome (59) using Bowtie (62)  
571 (Version 1.1.2) with no mismatches allowed, and discarding reads that could map in more than  
572 one location. In a typical experiment, more than 90% of reads were mapped to unique sites.  
573 After subtracting TA insertion sites in genes found to be essential under our conditions, the *G.*  
574 *sulfurreducens* genome contains about 55,000 sites where the *mariner* transposon could insert  
575 and produce viable mutants. As we also discounted insertions in the first 5% of a feature, as  
576 these often do not produce a knockout phenotype (27), libraries recovered insertions in over  
577 64% of available genomic TA sites that could produce viable mutants, providing an average of  
578 nearly 10 independent mutants per gene feature.

579  
580 Approximately 2.7% of the insertional reads mapped to more than one location in the *G.*  
581 *sulfurreducens* genome due to redundancies. Of interest to our analysis, the *omcB* (GSU2738 –  
582 GSU2737) and *omcC* (GSU2735 – GSU2731) gene clusters are tandemly duplicated in the  
583 genome. Two genes in each cluster are 99-100% identical (GSU2739-8 and GSU2733-2) at the

584 nucleotide level, preventing unique readsmapping to these genes, while the 12-heme  
585 cytochrome genes *omcB* (GSU2737) and *omcC* (GSU2731) share 87% DNA sequence identity  
586 and contained a few characteristic sites. When the 20 bp Mmel-generated genomic DNA reads  
587 mapped ambiguously to more than one site, they were excluded from analysis, and genes  
588 containing such sites were flagged to account for possible “low insertion density” in the gene  
589 that would wrongly code it as essential. Similar issues limited the amount of useful data for the  
590 small triheme cytochromes encoded in *ppcA-E* because there are few unique 20 bp regions in  
591 these small genes adjacent to TA sites. However, most ambiguous reads mapped to the 35  
592 transposable elements and duplicated ribosomal RNA genes. All ambiguous mappings were  
593 excluded from the essentiality analysis, but were included for total read normalization between  
594 barcoded libraries.

595  
596 To estimate the severity of a phenotype, the effective change in doubling times for Tn-Seq  
597 mutants was calculated. The exponential growth equation was applied using the WT doubling  
598 time of 10 hours for the duration of electrode growth (72 hours), comparing the reads in a gene  
599 between electrode and fumarate conditions where  $x$  is the apparent electrode growth doubling  
600 time (hours). According to the conditions of the experiment, a  $\text{Log}_2$  ration of -2 after 72 hours  
601 implies a mutant with a doubling time of ~15 hours.

$$\frac{\text{Reads}(\text{electrode})}{\text{Reads}(\text{parent})} = \frac{e^{\frac{\ln(2)}{x} * 72}}{e^{\frac{\ln(2)}{10} * 72}}$$

602 All of the Tn-Seq library sequence manipulations were performed in a Galaxy server hosted on  
603 the Minnesota Supercomputing Institute at the University of Minnesota (63).

604  
605 **Scarless gene deletion in *G. sulfurreducens*.** Roughly 1 kb flanking the targeted gene(s) of  
606 interest were cloned into the *sacB* encoding pK18mobsacB plasmid. To prevent disruption of

607 the flanking genes, about 30 bp of the target gene sequence coding for a small peptide was  
608 cloned within the flanking region. The *sacB* plasmid was transformed into *E. coli* conjugative  
609 donor strain S17-1 to conjugate into *G. sulfurreducens* recipient. One ml of fully grown *G.*  
610 *sulfurreducens* acetate-fumarate culture was pelleted on top of 1 ml of S17-1 culture carrying  
611 the *sacB* plasmid, mixed on top of a 0.22  $\mu$ m filter resting on acetate-fumarate agar plates in an  
612 anaerobic chamber and incubated for 4 hours before streaking the mixture onto acetate-  
613 fumarate plates with 200  $\mu$ g/ml kanamycin. This procedure selected *G. sulfurreducens* culture  
614 with pK18mobsacB integrated into either flanking region of the gene since the plasmid cannot  
615 replicate in *G. sulfurreducens*. Scarless gene deletion mutant was selected on acetate-fumarate  
616 plates containing 10% sucrose and confirmed using PCR with primers flanking the deletion site  
617 (59). The primers used to clone the flanking regions into pK18mobsacB and flanking primers to  
618 confirm gene deletions are listed in Table S1.

619  
620 **Tn-Seq raw sequencing data.** Illumina sequence data trimmed to remove transposon  
621 sequences and barcode sequences, containing only genomic DNA (.fastq) from each condition  
622 are deposited in NCBI short read archives with the following accession number: SRX2199236  
623 (fumarate outgrowth, used for determining essentiality), SRX2199234 (parent library, used as  
624 the reference to compare between fumarate and electrode conditions), and SRX2199233  
625 (concatenated with fastq headers HJHKHADXX and HJF5FADXX for electrode outgrowth  
626 replicates). Mapping files (.bam) for the fumarate outgrowth dataset used to determine  
627 essentiality is deposited as SRX2199235. The reference *G. sulfurreducens* genome used for all  
628 mapping was re-sequenced and deposited as SRX1101230. Instructions to view read mapping  
629 against our reference genome using IGV is available in supplemental file S7.

630

631

632



633 **Acknowledgements**

634 We thank M. Mehta for initiating the construction and analysis of preliminary Tn-Seq  
635 experiments in *G. sulfurreducens*. We thank J. Badalamenti for sequence analysis assistance  
636 and data management.

637

638 **Funding information**

639 This study was supported by grants N000141210308 and N000141612194 from the Office of  
640 Naval Research. F. Jimenez-Otero was supported by the Mexican National Council for Science  
641 and Technology C.E. Levar was supported by the State of Minnesota-University of Minnesota  
642 MNDrive program.

643

644

645

646

## 647 **References**

- 648 1. **Nealson KH, Saffarini D.** 1994. Iron and manganese in anaerobic respiration:  
649 environmental significance, physiology, and regulation. *Annu Rev Microbiol* **48**:311–343.
- 650 2. **Richter K, Schicklberger M, Gescher J.** 2012. Dissimilatory reduction of extracellular  
651 electron acceptors in anaerobic respiration. *Appl Environ Microbiol* **78**:913–921.
- 652 3. **Bond DR, Lovley DR.** 2003. Electricity production by *Geobacter sulfurreducens* attached  
653 to electrodes. *Appl Environ Microbiol* **69**:1548–1555.
- 654 4. **Wrighton KC, Thrash JC, Melnyk RA, Bigi JP, Byrne-Bailey KG, Remis JP, Schichnes**  
655 **D, Auer M, Chang CJ, Coates JD.** 2011. Evidence for direct electron transfer by a Gram-  
656 positive bacterium isolated from a microbial fuel cell. *Appl Environ Microbiol* **77**:7633–  
657 7639.
- 658 5. **Rotaru A-E, Shrestha PM, Liu F, Shrestha M, Shrestha D, Embree M, Zengler K,**  
659 **Wardman C, Nevin KP, Lovley DR.** 2013. A new model for electron flow during anaerobic  
660 digestion: direct interspecies electron transfer to *Methanosaeta* for the reduction of carbon  
661 dioxide to methane. *Energy Environ Sci* **7**:408–415.
- 662 6. **Rotaru A-E, Shrestha PM, Liu F, Markovaite B, Chen S, Nevin KP, Lovley DR.** 2014.  
663 Direct interspecies electron transfer between *Geobacter metallireducens* and  
664 *Methanosarcina barkeri*. *Appl Environ Microbiol* **80**:4599–4605.
- 665 7. **Breuer M, Rosso KM, Blumberger J, Butt JN.** 2015. Multi-haem cytochromes in  
666 *Shewanella oneidensis* MR-1: structures, functions and opportunities. *J R Soc Interface*  
667 **12**:20141117.

- 668 8. **Coursolle D, Baron DB, Bond DR, Gralnick JA.** 2010. The Mtr respiratory pathway is  
669 essential for reducing flavins and electrodes in *Shewanella oneidensis*. J Bacteriol  
670 **192**:467–474.
- 671 9. **Zacharoff L, Chan CH, Bond DR.** 2016. Reduction of low potential electron acceptors  
672 requires the CbcL inner membrane cytochrome of *Geobacter sulfurreducens*.  
673 Bioelectrochemistry Amst Neth **107**:7–13.
- 674 10. **Levar CE, Chan CH, Mehta-Kolte MG, Bond DR.** 2014. An inner membrane cytochrome  
675 required only for reduction of high redox potential extracellular electron acceptors. mBio  
676 **5**:e02034-14.
- 677 11. **Morgado L, Bruix M, Pessanha M, Londer YY, Salgueiro CA.** 2010. Thermodynamic  
678 characterization of a triheme cytochrome family from *Geobacter sulfurreducens* reveals  
679 mechanistic and functional diversity. Biophys J **99**:293–301.
- 680 12. **Liu Y, Wang Z, Liu J, Levar C, Edwards MJ, Babauta JT, Kennedy DW, Shi Z, Beyenal**  
681 **H, Bond DR, Clarke TA, Butt JN, Richardson DJ, Rosso KM, Zachara JM,**  
682 **Fredrickson JK, Shi L.** 2014. A trans-outer membrane porin-cytochrome protein complex  
683 for extracellular electron transfer by *Geobacter sulfurreducens* PCA. Environ Microbiol Rep  
684 **6**:776–785.
- 685 13. **Liu Y, Fredrickson JK, Zachara JM, Shi L.** 2015. Direct involvement of *ombB*, *omaB*,  
686 and *omcB* genes in extracellular reduction of Fe(III) by *Geobacter sulfurreducens* PCA.  
687 Front Microbiol **6**.
- 688 14. **Rollefson JB, Stephen CS, Tien M, Bond DR.** 2011. Identification of an extracellular  
689 polysaccharide network essential for cytochrome anchoring and biofilm formation in  
690 *Geobacter sulfurreducens*. J Bacteriol **193**:1023–1033.

- 691 15. **Mehta T, Coppi MV, Childers SE, Lovley DR.** 2005. Outer membrane c-type  
692 cytochromes required for Fe(III) and Mn(IV) oxide reduction in *Geobacter sulfurreducens*.  
693 *Appl Environ Microbiol* **71**:8634–8641.
- 694 16. **Reguera G, Pollina RB, Nicoll JS, Lovley DR.** 2007. Possible nonconductive role of  
695 *Geobacter sulfurreducens* pilus nanowires in biofilm formation. *J Bacteriol* **189**:2125–2127.
- 696 17. **Leang C, Coppi MV, Lovley DR.** 2003. OmcB, a c-type polyheme cytochrome, involved in  
697 Fe(III) reduction in *Geobacter sulfurreducens*. *J Bacteriol* **185**:2096–2103.
- 698 18. **Leang C, Lovley DR.** 2005. Regulation of two highly similar genes, *omcB* and *omcC*, in a  
699 10 kb chromosomal duplication in *Geobacter sulfurreducens*. *Microbiology* **151**:1761–  
700 1767.
- 701 19. **Barquist L, Boinett CJ, Cain AK.** 2013. Approaches to querying bacterial genomes with  
702 transposon-insertion sequencing. *RNA Biol* **10**:1161–1169.
- 703 20. **Sarmiento F, Mrázek J, Whitman WB.** 2013. Genome-scale analysis of gene function in  
704 the hydrogenotrophic methanogenic archaeon *Methanococcus maripaludis*. *Proc Natl*  
705 *Acad Sci U S A* **110**:4726–4731.
- 706 21. **Pechter KB, Gallagher L, Pyles H, Manoil CS, Harwood CS.** 2016. Essential genome of  
707 the metabolically versatile Alphaproteobacterium *Rhodopseudomonas palustris*. *J Bacteriol*  
708 **198**:867–876.
- 709 22. **Brutinel ED, Gralnick JA.** 2012. Anomalies of the anaerobic tricarboxylic acid cycle in  
710 *Shewanella oneidensis* revealed by Tn-seq. *Mol Microbiol* **86**:273–283.

- 711 23. **Bouhenni R, Gehrke A, Saffarini D.** 2005. Identification of genes involved in cytochrome  
712 *c* biogenesis in *Shewanella oneidensis*, using a modified *mariner* transposon. *Appl Environ*  
713 *Microbiol* **71**:4935–4937.
- 714 24. **van Opijnen T, Bodi KL, Camilli A.** 2009. Tn-seq: high-throughput parallel sequencing for  
715 fitness and genetic interaction studies in microorganisms. *Nat Methods* **6**:767–772.
- 716 25. **Lampe DJ, Grant TE, Robertson HM.** 1998. Factors affecting transposition of the *Himar1*  
717 *mariner* transposon *in vitro*. *Genetics* **149**:179–187.
- 718 26. **Mahadevan R, Bond DR, Butler JE, Esteve-Nuñez A, Coppi MV, Palsson BO,**  
719 **Schilling CH, Lovley DR.** 2006. Characterization of metabolism in the Fe(III)-reducing  
720 organism *Geobacter sulfurreducens* by constraint-based modeling. *Appl Environ Microbiol*  
721 **72**:1558–1568.
- 722 27. **Yang H, Krumholz EW, Brutinel ED, Palani NP, Sadowsky MJ, Odlyzko AM, Gralnick**  
723 **JA, Libourel IGL.** 2014. Genome-scale metabolic network validation of *Shewanella*  
724 *oneidensis* using transposon insertion frequency analysis. *PLoS Comput Biol* **10**.
- 725 28. **Spero MA, Aylward FO, Currie CR, Donohue TJ.** 2015. Phylogenomic analysis and  
726 predicted physiological role of the proton-translocating NADH:quinone oxidoreductase  
727 (complex I) across bacteria. *mBio* **6**:389–15.
- 728 29. **Chowdhury NP, Kahnt J, Buckel W.** 2015. Reduction of ferredoxin or oxygen by flavin-  
729 based electron bifurcation in *Megasphaera elsdenii*. *FEBS J* **282**:3149–3160.
- 730 30. **Kim B-C, Postier BL, Didonato RJ, Chaudhuri SK, Nevin KP, Lovley DR.** 2008.  
731 Insights into genes involved in electricity generation in *Geobacter sulfurreducens* via whole

- 732 genome microarray analysis of the OmcF-deficient mutant. *Bioelectrochemistry Amst Neth*  
733 **73:70–75.**
- 734 31. **Holmes DE, Chaudhuri SK, Nevin KP, Mehta T, Methé BA, Liu A, Ward JE, Woodard**  
735 **TL, Webster J, Lovley DR.** 2006. Microarray and genetic analysis of electron transfer to  
736 electrodes in *Geobacter sulfurreducens*. *Environ Microbiol* **8:1805–1815.**
- 737 32. **Majlan J, Navrotsky A, Schwertmann U.** 2004. Thermodynamics of iron oxides: Part III.  
738 Enthalpies of formation and stability of ferrihydrite ( $\sim\text{Fe}(\text{OH})_3$ ), schwertmannite  
739 ( $\sim\text{FeO}(\text{OH})_{3/4}(\text{SO}_4)_{1/8}$ ), and  $\epsilon\text{-Fe}_2\text{O}_3$  1. *Geochim Cosmochim Acta* **68:1049–1059.**
- 740 33. **Speers A, Schindler BD, Hwang J, Genc A, Reguera G.** 2016. Genetic identification of a  
741 PilT motor in *Geobacter sulfurreducens* reveals a role for pilus retraction in extracellular  
742 electron transfer. *Microb Physiol Metab* **7:1578.**
- 743 34. **Tran HT, Krushkal J, Antommattei FM, Lovley DR, Weis RM.** 2008. Comparative  
744 genomics of *Geobacter* chemotaxis genes reveals diverse signaling function. *BMC*  
745 *Genomics* **9:471.**
- 746 35. **Porter SL, Wadhams GH, Armitage JP.** 2011. Signal processing in complex chemotaxis  
747 pathways. *Nat Rev Microbiol* **9:153–165.**
- 748 36. **Zou SB, Hersch SJ, Roy H, Wiggers JB, Leung AS, Buranyi S, Xie JL, Dare K, Ibba M,**  
749 **Navarre WW.** 2012. Loss of elongation factor P disrupts bacterial outer membrane  
750 integrity. *J Bacteriol* **194:413–425.**
- 751 37. **Lassak J, Wilson DN, Jung K.** 2016. Stall no more at polyproline stretches with the  
752 translation elongation factors EF-P and IF-5A. *Mol Microbiol* **99:219–235.**

- 753 38. **Nevin KP, Kim B-C, Glaven RH, Johnson JP, Woodard TL, Methé BA, Didonato RJ,**  
754 **Covalla SF, Franks AE, Liu A, Lovley DR.** 2009. Anode biofilm transcriptomics reveals  
755 outer surface components essential for high density current production in *Geobacter*  
756 *sulfurreducens* fuel cells. PloS One **4**:e5628.
- 757 39. **Inoue K, Leang C, Franks AE, Woodard TL, Nevin KP, Lovley DR.** 2011. Specific  
758 localization of the *c*-type cytochrome OmcZ at the anode surface in current-producing  
759 biofilms of *Geobacter sulfurreducens*. Environ Microbiol Rep **3**:211–217.
- 760 40. **Summers ZM, Fogarty HE, Leang C, Franks AE, Malvankar NS, Lovley DR.** 2010.  
761 Direct exchange of electrons within aggregates of an evolved syntrophic coculture of  
762 anaerobic bacteria. Science **330**:1413–1415.
- 763 41. **Galushko AS, Schink B.** 2000. Oxidation of acetate through reactions of the citric acid  
764 cycle by *Geobacter sulfurreducens* in pure culture and in syntrophic coculture. Arch  
765 Microbiol **174**:314–321.
- 766 42. **Ducret A, Fleuchot B, Bergam P, Mignot T.** 2013. Direct live imaging of cell-cell protein  
767 transfer by transient outer membrane fusion in *Myxococcus xanthus*. eLife **2**:e00868.
- 768 43. **Cordero OX, Ventouras L-A, DeLong EF, Polz MF.** 2012. Public good dynamics drive  
769 evolution of iron acquisition strategies in natural bacterioplankton populations. Proc Natl  
770 Acad Sci U S A **109**:20059–20064.
- 771 44. **Richter H, Nevin KP, Jia H, Lowy DA, Lovley DR, Tender LM.** 2009. Cyclic voltammetry  
772 of biofilms of wild type and mutant *Geobacter sulfurreducens* on fuel cell anodes indicates  
773 possible roles of OmcB, OmcZ, type IV pili, and protons in extracellular electron transfer.  
774 Energy Environ Sci **2**:506–516.

- 775 45. **Hallberg ZF, Wang XC, Wright TA, Nan B, Ad O, Yeo J, Hammond MC.** 2016. Hybrid  
776 promiscuous (Hypr) GGDEF enzymes produce cyclic AMP-GMP (3', 3'-cGAMP). *Proc Natl*  
777 *Acad Sci U S A* **113**:1790–1795.
- 778 46. **Römling U, Galperin MY, Gomelsky M.** 2013. Cyclic di-GMP: the first 25 years of a  
779 universal bacterial second messenger. *Microbiol Mol Biol Rev* **77**:1–52.
- 780 47. **Ding Y-HR, Hixson KK, Giometti CS, Stanley A, Esteve-Núñez A, Khare T, Tollaksen**  
781 **SL, Zhu W, Adkins JN, Lipton MS, Smith RD, Mester T, Lovley DR.** 2006. The  
782 proteome of dissimilatory metal-reducing microorganism *Geobacter sulfurreducens* under  
783 various growth conditions. *Biochim Biophys Acta* **1764**:1198–1206.
- 784 48. **Franks AE, Nevin KP, Glaven RH, Lovley DR.** 2010. Microtoming coupled to microarray  
785 analysis to evaluate the spatial metabolic status of *Geobacter sulfurreducens* biofilms.  
786 *ISME J* **4**:509–519.
- 787 49. **Segura D, Mahadevan R, Juárez K, Lovley DR.** 2008. Computational and experimental  
788 analysis of redundancy in the central metabolism of *Geobacter sulfurreducens*. *PLoS*  
789 *Comput Biol* **4**.
- 790 50. **Rotaru A-E, Woodard TL, Nevin KP, Lovley DR.** 2015. Link between capacity for current  
791 production and syntrophic growth in *Geobacter* species. *Front Microbiol* **6**.
- 792 51. **Miceli JF, Parameswaran P, Kang D-W, Krajmalnik-Brown R, Torres CI.** 2012.  
793 Enrichment and analysis of anode-respiring bacteria from diverse anaerobic inocula.  
794 *Environ Sci Technol* **46**:10349–10355.
- 795 52. **Yokoyama H, Ishida M, Yamashita T.** 2016. Comparison of anodic community in  
796 microbial fuel cells with iron oxide-reducing community. *J Microbiol Biotechnol* **26**:757–762.



- 797 53. **Kato S, Hashimoto K, Watanabe K.** 2012. Methanogenesis facilitated by electric  
798 syntrophy via (semi)conductive iron-oxide minerals. *Environ Microbiol* **14**:1646–1654.
- 799 54. **Levar CE, Rollefson JB, Bond DR.** 2013. Energetic and molecular constraints on the  
800 mechanism of environmental Fe(III) reduction by *Geobacter*, p. 29–48. *In* Gescher, J,  
801 Kappler, A (eds.), *Microbial Metal Respiration*. Springer Berlin Heidelberg.
- 802 55. **Le Goff A, Holzinger M, Cosnier S.** 2015. Recent progress in oxygen-reducing laccase  
803 biocathodes for enzymatic biofuel cells. *Cell Mol Life Sci CMLS* **72**:941–952.
- 804 56. **Foley JM, Rozendal RA, Hertle CK, Lant PA, Rabaey K.** 2010. Life cycle assessment of  
805 high-rate anaerobic treatment, microbial fuel cells, and microbial electrolysis cells. *Environ*  
806 *Sci Technol* **44**:3629–3637.
- 807 57. **Clauwaert P, Aelterman P, Pham TH, De Schampheleire L, Carballa M, Rabaey K,**  
808 **Verstraete W.** 2008. Minimizing losses in bio-electrochemical systems: the road to  
809 applications. *Appl Microbiol Biotechnol* **79**:901–913.
- 810 58. **Logan BE, Rabaey K.** 2012. Conversion of wastes into bioelectricity and chemicals by  
811 using microbial electrochemical technologies. *Science* **337**:686–690.
- 812 59. **Chan CH, Levar CE, Zacharoff L, Badalamenti JP, Bond DR.** 2015. Scarless genome  
813 editing and stable inducible expression vectors for *Geobacter sulfurreducens*. *Appl Environ*  
814 *Microbiol* **81**:7178–7186.
- 815 60. **Marsili E, Rollefson JB, Baron DB, Hozalski RM, Bond DR.** 2008. Microbial biofilm  
816 voltammetry: direct electrochemical characterization of catalytic electrode-attached  
817 biofilms. *Appl Environ Microbiol* **74**:7329–7337.

- 818 61. **van Opijnen T, Camilli A.** 2010. Genome-wide fitness and genetic interactions  
819 determined by Tn-seq, a high-throughput massively parallel sequencing method for  
820 microorganisms. *Curr Protoc Microbiol* 19:E:1E.3:1E.3.1–1E.3.16.
- 821 62. **Langmead B, Trapnell C, Pop M, Salzberg SL.** 2009. Ultrafast and memory-efficient  
822 alignment of short DNA sequences to the human genome. *Genome Biol* 10:R25.
- 823 63. **Afgan E, Baker D, van den Beek M, Blankenberg D, Bouvier D, Čech M, Chilton J,**  
824 **Clements D, Coraor N, Eberhard C, Grüning B, Guerler A, Hillman-Jackson J, Von**  
825 **Kuster G, Rasche E, Soranzo N, Turaga N, Taylor J, Nekrutenko A, Goecks J.** 2016.  
826 The Galaxy platform for accessible, reproducible and collaborative biomedical analyses:  
827 2016 update. *Nucleic Acids Res* 44:W3–W10.
- 828 64. **Simon R, Priefer U, Pühler A.** 1983. A broad host range mobilization system for *in vivo*  
829 genetic engineering: transposon mutagenesis in Gram negative bacteria. *Nat Biotechnol*  
830 1:784–791.

831  
832  
833  
834

835

836

837

838

839

840

841

842 **Figure Legends**

843

844 **Figure 1. Tn-Seq reproducibility within library replicates and between experimental**

845 **replicates in *Geobacter sulfurreducens*.** (A) Comparison of two subsamples of the same

846 fumarate-grown library. The number of reads mapped to a gene (normalized for read depth) is

847 plotted against data for the same gene prepared and sequenced in parallel. (B) Comparison of

848 two separate cultures inoculated on a poised electrode as terminal electron acceptor, recovered

849 and sequenced separately.

850

851 **Figure 2. Estimation of essential genes based on low insertion densities, and use of *in***

852 ***silico* model data to verify essentiality predictions.** (A) The frequency distribution for

853 fumarate-grown cells follows a bimodal distribution centered around 10 insertions/kb, with

854 strong enrichment below 4 insertions per kb (left of the dashed line). Genes with few insertions

855 are predicted to be essential under these conditions. (B) Most genes labeled as essential in *in*

856 *silico* modeling also contained less than 4 insertion sites per kb, and had less than 300 mapped

857 reads/gene (26).

858

859 **Figure 3. Genes essential for growth with electrodes are not required for Fe(III) reduction.**

860 Growth of scarless deletion mutants of chemosensory-like genes *esnA*, *esnB*, *esnC* and *esnD*

861 and extracellular conduit clusters *extABCD*, *omcBC*, *extEFG* and *extHIJKL* with (A) insoluble

862 Fe(III) oxides and (B) poised electrodes. The amount of Fe(III) reduced in 7 days was

863 normalized to WT. Maximum current densities on electrodes poised at -0.1 V vs. SHE were

864 recorded for all strains 80 hours after inoculation. All experiments were performed in triplicate.

865

866

867

868 **Table 1. Strains and plasmids used in this work**

869

Strain or Plasmid	Description or relevant genotype	Source or reference
<i>G. sulfurreducens</i> strains		
DB823	$\Delta esnA$ ( $\Delta$ GSU1704)	This study
DB836	$\Delta esnB$ ( $\Delta$ GSU2220)	This study
DB824	$\Delta esnC$ ( $\Delta$ GSU2222)	This study
DB1130	$\Delta esnD$ ( $\Delta$ GSU3376)	This study
DB1280	$\Delta extABCD$ ( $\Delta$ GSU2645-GSU2642)	This study
DB1282	$\Delta extEFG$ ( $\Delta$ GSU2726-GSU2724)	This study
DB1279	$\Delta omcBC$ cluster ( $\Delta$ GSU2739-GSU2731)	This study
DB1281	$\Delta extHIJKL$ ( $\Delta$ GSU2940-GSU2936)	This study
<i>E. coli</i> strains		
S17-1	<i>recA pro hsdR RP4-2-Tc::Mu-Km::Tn7</i>	(64)
BW29427 (WM3064)	<i>thrB1004 pro thi rpsL hsdS lacZ<math>\Delta</math>M15 RP4-1360</i> $\Delta(araBAD)567 \Delta dapA1341::[erm\ pir]$	K. Datsenko and B. L. Wanner
Plasmids		
pEB001	Plasmid carrying mini <i>Himar</i> RB1 transposon with engineered Mmel restriction sites	(22)
pK18mobsacB	SacB encoding scarless deletion vector	(64)
pDGSU1704	Flanking regions of GSU1704 in pK18mobsacB	This study
pDGSU2220	Flanking regions of GSU2220 in pK18mobsacB	This study
pDGSU2222	Flanking regions of GSU2222 in pK18mobsacB	This study
pDGSU3376	Flanking regions of GSU3376 in pK18mobsacB	This study
pDGSU2645-2642	Flanking regions of GSU2645-2642 in pK18mobsacB	This study
pDGSU2726-2724	Flanking regions of GSU2726-2724 in pK18mobsacB	This study
pDGSU2739-2731	Flanking regions of GSU2739-2731 in pK18mobsacB	This study
pDGSU2940-2936	Flanking regions of GSU2940-2936 in pK18mobsacB	This study

870  
871  
872  
873  
874  
875  
876  
877  
878  
879  
880  
881  
882  
883  
884  
885  
886

887 **Table 2.** TnSeq mutations which after growth on an electrode showed a decrease in reads  
 888 mapped by at least a Log<sub>2</sub> ratio of -2, equivalent to a predicted 50% reduction in growth rate.  
 889

Locus	Gene symbol and description	Log <sub>2</sub> ratio
<b>Cytochrome</b>		
GSU0274	<i>cbcl</i> , <i>c</i> - and <i>b</i> -type cytochrome	-3.3
GSU2643	<i>extC</i> , lipoprotein cytochrome <i>c</i>	-2.0
GSU2645	<i>extA</i> , cytochrome <i>c</i>	-2.5
<b>Metabolism and protein processing</b>		
GSU0140	phosphoribosylaminoimidazole carboxylase-like protein	-2.2
GSU0503	<i>crcB</i> , camphor resistance protein CrcB	-2.2
GSU0536	adenosine nucleotide alpha-hydrolase superfamily protein	-2.6
GSU0994	<i>fumB</i> , fumarate hydratase	-8.0
GSU1105	prolidase family protein	-2.0
GSU1279	<i>nikMN</i> , nickel ABC transporter membrane protein NikMN	-2.0
GSU1752	<i>efp-2</i> , elongation factor P	-2.5
GSU1753	<i>genX</i> , translation elongation factor P-lysine lysyltransferase	-2.9
GSU1754	<i>yjeK</i> , translation elongation factor P-lysyl-lysine 2,3-aminomutase	-2.8
GSU3278	pentapeptide repeat-containing protein	-2.0
<b>Signaling and regulation</b>		
GSU0013	MarR family winged helix-turn-helix transcriptional regulator	-2.1
GSU1704	<i>esnA</i> , GAF sensor methyl-accepting chemotaxis sensory transducer, class 40H	-2.4
GSU2220	<i>esnB</i> , scaffold protein CheW associated with MCPs of class 40H	-2.4
GSU2221	ATPase	-2.1
GSU2222	<i>esnC</i> , sensor histidine kinase CheA associated with MCPs of class 40H	-2.8 <sup>a</sup>
<b>Extracellular structures</b>		
GSU1114	lipoprotein	-2.1
GSU1493	<i>pilC</i> , type IV pilus inner membrane protein PilC	-2.2
GSU1494	<i>pilS</i> , sensor histidine kinase PilS, PAS domain-containing	-2.2
GSU1501	<i>xapD</i> , ABC transporter ATP-binding protein	-2.0
GSU1816	<i>ugd</i> , UDP-glucose 6-dehydrogenase	-2.0
GSU1889	<i>lptA</i> , lipopolysaccharide ABC transporter periplasmic protein LptA	-6.5
GSU1976	YqgM-like family glycosyltransferase	-4.9
GSU2028	<i>pilQ</i> , type IV pilus secretin lipoprotein PilQ	-2.5
GSU2029	<i>pilP</i> , type IV pilus assembly lipoprotein PilP	-3.3
GSU2030	<i>pilO</i> , type IV pilus biogenesis protein PilO	-2.5
GSU2032	<i>pilM</i> , type IV pilus biogenesis ATPase PilM	-2.4
GSU2085	<i>hldE</i> , D-glycero-D-mannoheptose-7-phosphate kinase and D-glycero-D-mannoheptose-1-phosphate adenylyltransferase	-3.1
GSU2087	<i>gmhA</i> , phosphoheptose isomerase	-3.7
GSU2973	lipoprotein	-2.7
GSU3321	phosphoglucomutase/phosphomannomutase family protein	-2.2
<b>Hypothetical</b>		
GSU2086	hypothetical protein	-3.2
GSU2713	hypothetical protein	-2.9
GSU2257	hypothetical protein	-2.4
GSU0141	hypothetical protein	-2.3
GSU0959	hypothetical protein	-2.3
GSU2048	hypothetical protein	-2.1

890

891 <sup>a</sup> coded as essential in our study

892

## Figure 1

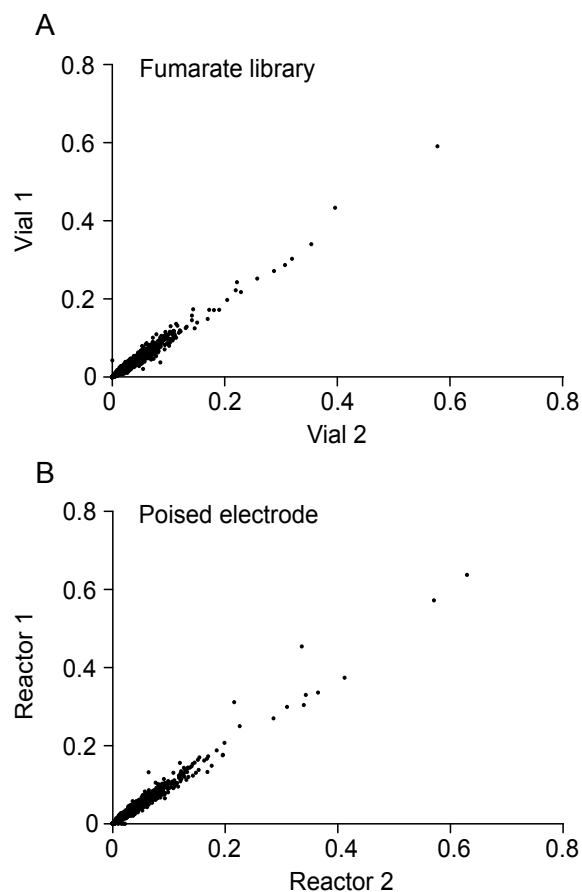


**Figure 1. Tn-Seq reproducibility within library replicates and between experimental replicates in *Geobacter sulfurreducens*.** (A) Comparison of two subsamples of the same fumarate-grown library. The number of reads mapped to a gene (normalized for read depth) is plotted against data for the same gene prepared and sequenced in parallel. (B) Comparison of two separate cultures inoculated on a poised electrode as terminal electron acceptor, recovered and sequenced separately.

## Figure 2

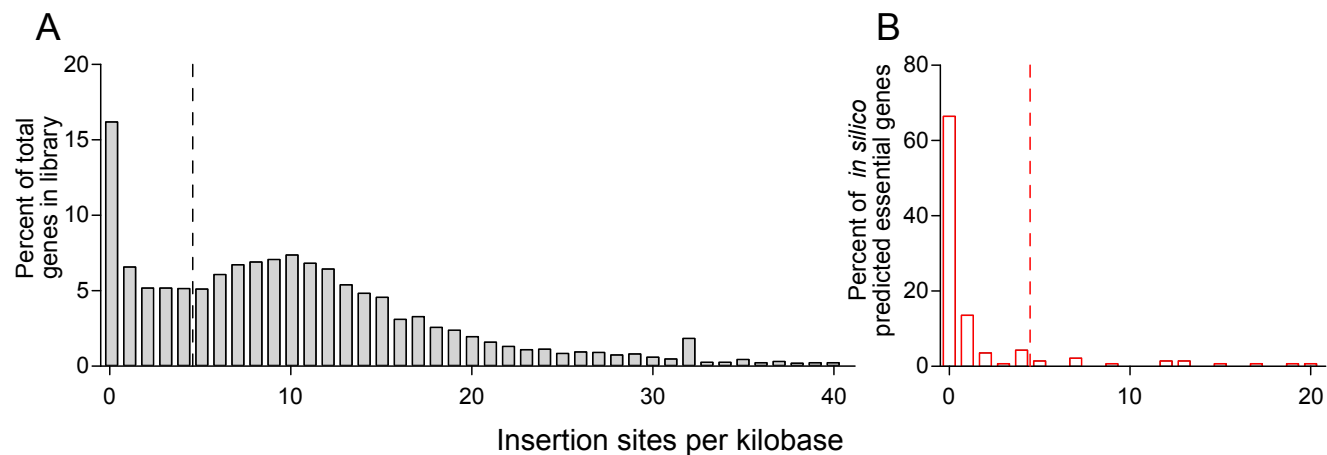


**Figure 2. Estimation of essential genes based on low insertion densities, and use of *in silico* model data to verify essentiality predictions.** (A) The frequency distribution for fumarate-grown cells follows a bimodal distribution centered around 10 insertions/kb, with strong enrichment below 4 insertions per kb (left of the dashed line). Genes with few insertions are predicted to be essential under these conditions. (B) Most genes labeled as essential in *in silico* modeling also contained less than 4 insertion sites per kb, and had less than 300 mapped reads/gene (26).

## Figure 3

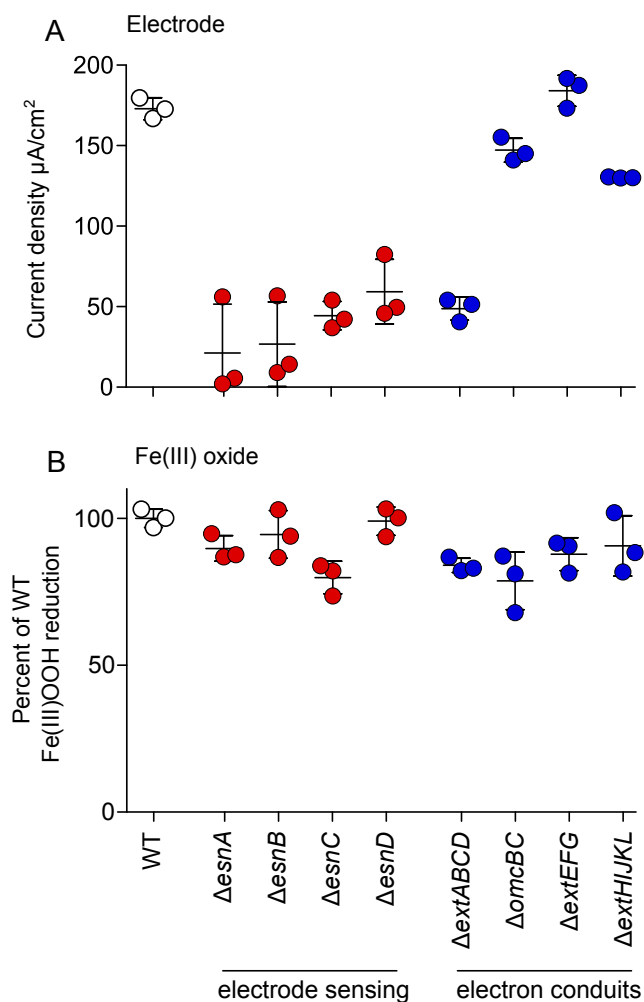


**Figure 3. Genes essential for growth with electrodes are not required for Fe(III) reduction.** Growth of scarless deletion mutants of chemosensory-like genes *esnA*, *esnB*, *esnC* and *esnD* and extracellular conduit clusters *extABCD*, *omcBC*, *extEFG* and *extHIJKL* with (A) insoluble Fe(III) oxides and (B) poised electrodes. The amount of Fe(III) reduced in 7 days was normalized to WT. Maximum current densities on electrodes poised at -0.1 V vs. SHE were recorded for all strains 80 hours after inoculation. All experiments were performed in triplicate.